

FEASIBILITY STUDY OF A TECHNOLOGICAL DEMONSTRATOR OF REDUCED SIZE FOR SUB-ORBITAL FLIGHT

S. Chiesa*, S. Corpino*, N. Viola*

*Department of Aeronautics and Space Engineering
Politecnico di Torino

Corso Einaudi, 40, 10129 Torino, Italy
+39-011-5646858

sergio.chiesa@polito.it; sabrina.corpino@polito.it; nicole.viola@polito.it

Keywords: *technological demonstrator, systems design, mission simulation*

Abstract

The Unmanned Space Vehicles program (USV), managed by the Italian Aerospace Research Centre (CIRA), is a science and technology knowledge development program, oriented towards future generations of Reusable Launch Vehicles, capable of performing frequent, and affordable launches into space [1]. The USV program has been defined based on the belief that future space access and re-entry will be guaranteed by aviation-like vehicles. The USV program therefore aims at the development of innovative technologies for future space vehicles. The program pursues an approach characterized by increasing mission complexity: three Flying Test Beds (FTBs) will be designed and built to perform four experimental flight tests. The planned missions are: Dropped Transonic Flight Test (DTFT), Sub-orbital Re-entry Test (SRT), Hypersonic Flight Test (HFT) and Orbital Re-entry Test (ORT). As these FTBs are thought as vehicles of considerable size, about 7.5 meters long, the study and development of smaller technological demonstrators, conceived to lead to the realization of bigger ones, appear attractive thanks to their high benefit-to-cost ratio. The aerospace system research group at Politecnico di Torino has been working at the design of small and affordable technological demonstrators for many years now and different configurations have been developed [2] [3] [4]. In collaboration with CIRA, Università di Napoli "Federico II" and Università di Roma

"La Sapienza", our research group has carried out the feasibility study of a small vehicle oriented towards the execution of the SRT mission. The vehicle has been called "Mini-FTB" and its mission "Mini-SRT". The CIRA demonstrator for the original SRT mission (FTB_2) is powered by one solid rocket engine. It will be dropped from a stratospheric balloon at an altitude of about 35 km. After that, the rocket is ignited to accelerate the vehicle along a sub-orbital trajectory up to a maximum altitude of about 120 km. Then the vehicle starts the re-entry phase along a trajectory designed to maximize heat fluxes, that remain higher than 650 kW/sqm for about 15 seconds, achieving the maximum value at about 25 km. A parachute system allows the recovery of the vehicle.

Main target of the Mini-SRT mission is to improve technological and scientific knowledge useful to reduce risks connected to the SRT mission by means of a low cost and thus low risk system. The result is encouraging as the feasibility study has shown that the Mini-FTB can be built and tested.

1 An overview of the design process

The flow chart of the design process is illustrated in figure 1. The result of the feasibility study [5] has been the complete definition of two configurations of the demonstrator: Mini-FTB (figure 2) and Mini-FTB/A (figure 3). The main difference between the two versions is the propulsion system

adopted: in fact, while Mini-FTB uses the rocket engine ATK STAR17, the Mini-FTB/A employs the ATK STAR17A, characterized by higher performances. Another difference between the two versions is the possibility for Mini-FTB of choosing between two types of cold gas for the RCS system, Nitrogen and Freon-14.

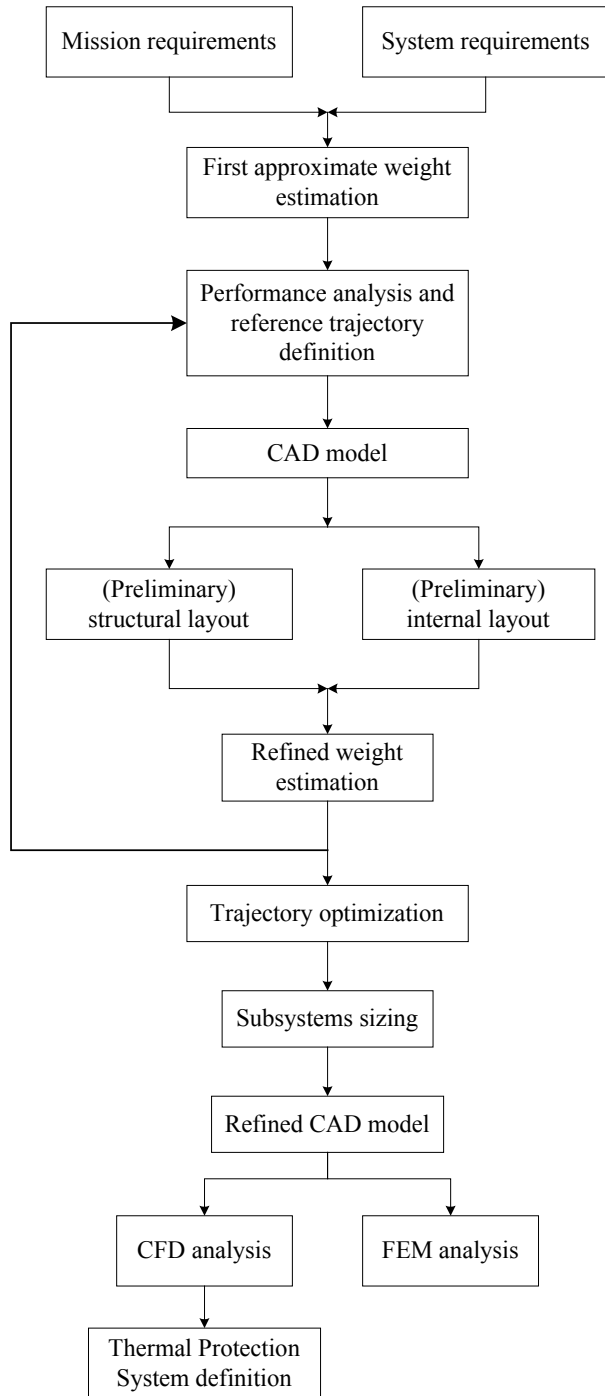


Fig. 1: design process flow chart

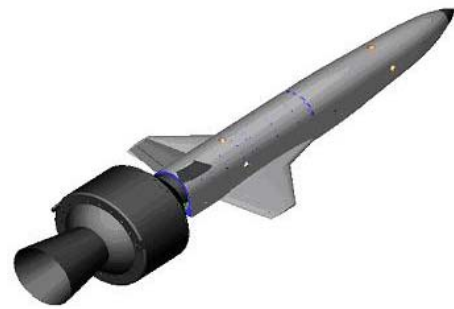


Fig. 2: Mini-FTB (STAR17)

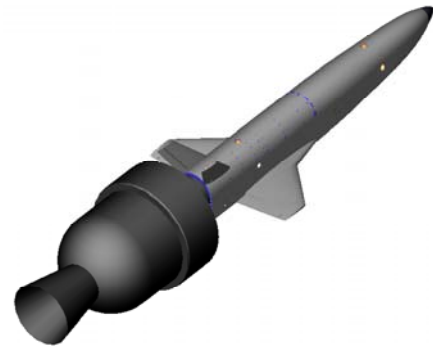


Fig. 3: Mini-FTB/A (STAR17A)

2 Requirements

2.1 Mission requirements

Mini-SRT mission requirements are listed as follows:

- sub-orbital flight: Mini-FTB has to perform a sub-orbital flight characterized by autonomous flight capability;
- data acquisition: Mini-FTB has to be able to perform data acquisition, processing and transmission, in order to support onboard operations, ground tracking of the flight and post flight analyses;
- sub-orbital ceiling height: the ceiling height requirement of 120 km or more must be met;
- thermal conditions during atmospheric flight: the maximum heat flux density requirement of 350 kW/m² or more must be met and sustained for at least 15 seconds;
- transonic flight: the requirement of 1÷1.1 Mach at 10÷15 km has to be met during re-entry;

- launch base: Trapani-Milo has to be considered as launch site of reference;
 - altitude at vehicle's release: the nominal altitude allowed for vehicle's release from the carrier has to be higher than 20 km;
 - safe separation between the vehicle and its carrier;
 - radio link: radio uplink and downlink between the Mini-FTB and the ground station has to be available during the overall mission;
 - landing phase: the vehicle's third stage, i.e. the Mini-FTB without its rocket engine, has to be recovered after its splash down;
 - parachute system opening: the parachute has to be deployed at a speed lower than 0.6 Mach and at an altitude higher than 10000 m to allow for a safe deceleration phase;
 - parachute system opening point dispersion: considering the splash down target, the parachute opening point of the third stage has to lay in the following ranges: ± 20 km of long range and ± 10 km of cross range. The occurrence of a larger ground dispersion area entails that the mission has been degraded;
 - Mini-FTB reusability: the Mini-FTB has to be designed and manufactured to be recovered but not to be completely reusable;
 - dynamic pressure: the maximum dynamic pressure requirement of 130 kPa has to be met during re-entry.
- system has to be able to provide the Mini-FTB with the total impulse necessary to reach the required sub-orbital conditions;
 - reaction control system (RCS): the Mini-FTB has to perform autonomous attitude control by means of a reaction control system, which has to be used both for the boosted and the ballistic phase. The RCS ought to be a cold gas system;
 - aerodynamic flight control surfaces: the Mini-FTB has to perform autonomous flight and attitude control by means of aerodynamic control surfaces when it is possible;
 - thermal protection system (TPS): the Mini-FTB has to be equipped with a TPS, if it is necessary;
 - parachute load: the maximum force at parachute's deployment has to be lower than 75 kN;
 - project cost: Mini-FTB has to be a low cost system. Thus it must use COTS equipments and state of the art technologies;
 - wing loading similitude: in order to meet the wing loading similitude between Mini-FTB and FTB_2, Mini-FTB has to weight about 50 kilograms during re-entry;
 - inertial loads similitude: in order to meet the inertial loads similitude between Mini-FTB and FTB_2 during re-entry, the values of the Mini-FTB principal moments of inertia has to be as follows: J_1 (pitch)= $10 \pm 20\%$ kg·m², J_2 (yaw)= $10.4 \pm 20\%$ kg·m², J_3 (roll)= $0.8 \pm 20\%$ kg·m².

2.2 System requirements

Mini-FTB system requirements are listed as follows:

- launch configuration: Mini-SRT mission has to be performed by the following three stages: the carrier, constituted by a stratospheric balloon, as first stage, the Mini-FTB with its booster as second stage and the Mini-FTB alone as third stage;
- Mini-FTB shape: the Mini-FTB and the FTB_2 has to be drawn to 1:5 scale;
- propulsion system: the Mini-FTB has to be equipped with an external propulsion system to be activated after the Mini-FTB has been released from the carrier. The propulsion

3 Mission profile and simulation

3.1 Mission profile

The proposed mission profile is here illustrated:

- pre-flight operations;
- launch of the whole system, constituted by the stratospheric balloon, the nacelle, the Mini-FBT and its engine, from Trapani-Milo base;
- heating of the Mini-FTB and its engine during the ascent phase;

- on-board systems' bootstrap and booting of the inertial platform just before the Mini-FTB is released from the carrier;
- heading control by means of the RCS system;
- at the nominal release altitude, checking of the correct trim and starting of the countdown;
- mechanical separation between the nacelle and the second stage;
- free dropping of the second stage for one second;
- engine ignition (11 kN thrust for 18 second). The RCS system makes the demonstrator follow the nominal climb trajectory, allowing the demonstrator reach sub-orbital condition (about 120 Km altitude in accordance with the sub-orbital ceiling height requirement);
- engine cut off and separation between the Mini-FTB and the engine itself;
- ballistic trajectory. The attitude control system operates in impulsive mode;
- re-entry phase, where maximum thermal loads are reached;
- parachute system's deployment at Mach < 0.6 and at 10000 m of height;
- Mini-FTB splashdown;
- Mini-FTB recovery.

3.2 Mission simulation

The mission simulation results show that the proposed flight profile is feasible and compliant with the mission requirements, as figure 4 illustrates for the dynamic pressure requirement.

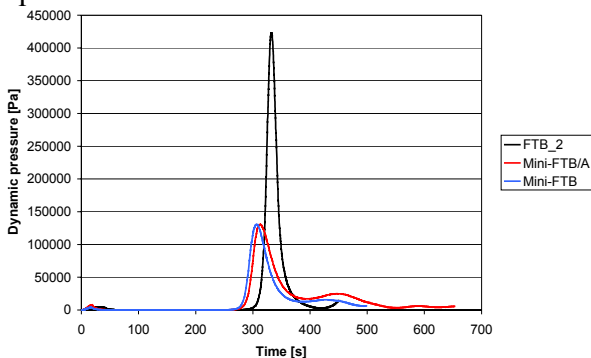


Fig. 4: dynamic pressure's values comparison

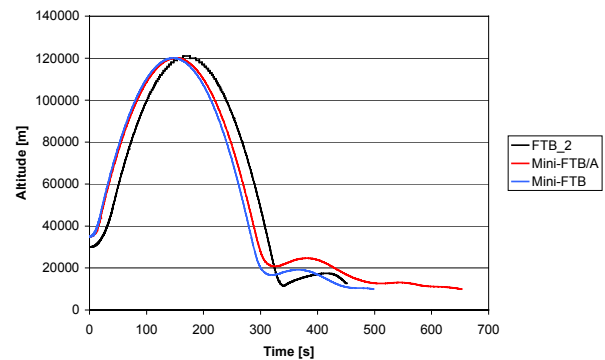


Fig. 5: trajectory comparison

Figure 5 shows the comparison between the Mini-FTB, Mini-FTB/A and the FTB_2 trajectory.

4 Configuration

The external configuration of Mini-FTB and FTB_2 are the same. Except for some details, Mini-FTB and FTB_2 are drawn to 1:5 scale. The rear part of the Mini-FTB has been partially modified with respect to FTB_2 in order to allow the external propulsion system's installation. The nose is designed to be interchangeable. It is possible for the nose to maintain the same shape of the one of FTB_2 (1:5 scale) to test aerodynamic characteristics. Conversely, it is possible for the nose radius to be drawn to a different scale to test materials under severe conditions.

Mini-FTB main characteristics are:

scale:	1:5
length:	1.6 m
wing span:	0.71 m
reference wing area:	0.14 m ²
fuselage height:	0.19 m
fuselage width:	0.2 m
maximum height (empennages):	0.32 m
shape:	similar to FTB_2
basic material:	Incoloy® MA956 (TPS substrate)/AISI 316 steel (structure)
TPS:	TBC and/or Ceramic Matrix Composites (CMC)

Figure 6, 7 and 8 illustrate the Mini-FTB 3D CAD model [6].



Fig. 6: side view of the Mini-FTB



Fig. 7: side view of the Mini-FTB and its propulsion system

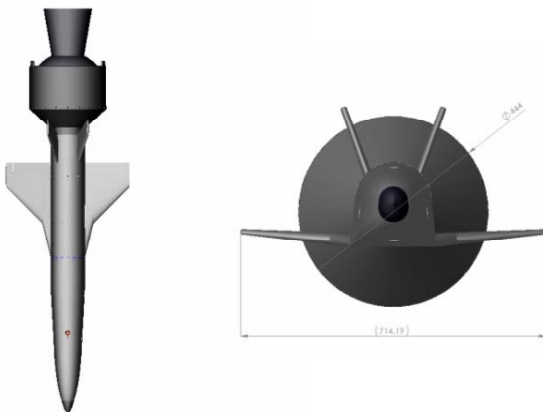


Fig. 8: upper and front view of the Mini-FTB and its propulsion system

5 Structural design

The driving factor of Mini-FTB structural design, in compliance with the philosophy of the project, is to keep cost as low as possible to satisfy design requirements. Commercial off the shelf materials have been widely used, as well as state of the art technologies.

Mini-FTB has been designed to be constituted by four main parts (see figure 9) to be assembled: forward body, wing/main body, rear body/empennages, power system. Figure 10 illustrates the Mini-FTB structural layout without systems and external skin.

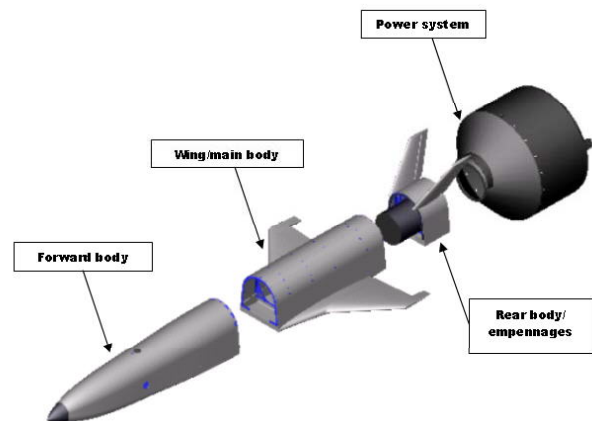


Fig. 9: Mini-FTB four main parts

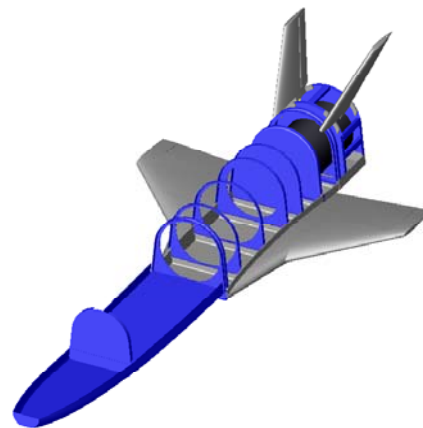


Fig. 10: Mini-FTB internal structure

6 Onboard systems

Taking into account safety, the philosophy of the onboard systems design has been to keep it simple in order to reduce design and manufacturing's time and cost.

To perform the mission, the Mini-FTB needs the following onboard subsystems: Power System (PS), Electrical Power System (EPS), Reaction Control System (RCS), Flight Control System (FCS), Data Handling System (DHS); Tracking Telecommunication and Control System (TT&C), Guidance Navigation and Control System (GN&C), Recovery System (RS). For all of them, reference off-the-shelf components have been chosen in order to confirm the feasibility and the availability of the whole system.

Figure 11 illustrates the Mini-FTB internal layout.

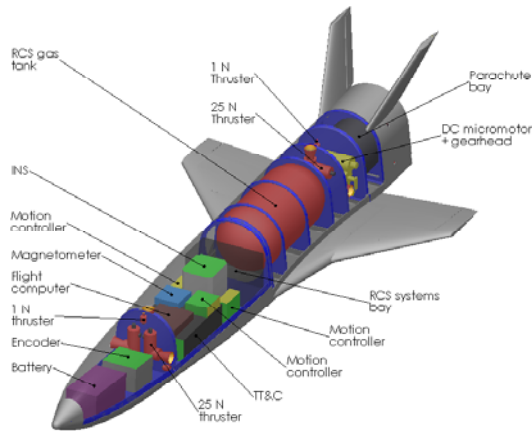




Fig. 11: Mini-FTB internal layout

6.1 Power system

In order to perform the mission, Mini-FTB is equipped by an expendable rocket motor produced by ATK Thiokol Propulsion. As already mentioned, both the STAR17 and STAR17A apogee kick engine models have been chosen. Their main characteristics are shown in tables 1 and 2.

Burn time:	17.6 s
Maximum thrust:	12348 N
Total impulse:	190.68 kNs
Weight (structure and propellant):	79.0 kg (84 kg with adapting structure)
Weight (propellant only):	69.6 kg
	

Tab. 1: STAR17 main characteristics

Burn time:	19 s
Medium thrust:	16810 N
Total impulse:	319.38 kNs
Weight (structure and propellant):	126.1 kg (131 kg with adapting structure)
Weight (propellant only):	112.2 kg
	

Tab. 2: STAR17A main characteristics

The STAR17 model is used for a less demanding mission. In order to improve performances the STAR17A model can be used (please note that, in this case, the demonstrator-engine attachment has to be modified). Unlike the power system of FTB_2, both STAR17 and STAR17A are not equipped by a TVC system. To overcome this drawback, the Reaction Control Systems has to be installed onboard the demonstrator and used during the boosted phase. Unlike the power system of FTB_2, which is placed inside the vehicle, the dimensions of the STAR17 and the STAR17A make it impossible to house the engine inside the demonstrator's body. Therefore an adapter is necessary (see figure 9). A good alternative to Thiokol's power systems is a commercial experimental engine for rocketry purposes (150 mm P hybrid motor). It employs peroxide of nitrogen as propellant: it is not dangerous and it is cheap, easily available and rechargeable. In order to achieve the same performance as with STAR17, three engines of this kind has to be used (figure 24).

6.2 Electrical Power System

The electrical power system is constituted by (figure 12): battery packages, one transformer and an electronic discharge control.

The Electrical Ground Support Equipments (EGSE) and the nacelle are used to provide electrical power respectively during pre-flight operations and during the ascent phase until the demonstrator is released from the balloon. Then, the onboard batteries become the main electrical power source for all flight. Onboard batteries supply 28 Volt (DC current). A transformer is thus necessary to supply 5 Volt for onboard electronics. A discharge electronic control device is useful to control and stabilize the current during battery discharge.

6.3 Reaction control system

Taking into account that the rocket engine does not have the TVC system, useful to maintain the nominal trajectory during the boosted phase notwithstanding the disturbance

torques which arise from the not-aligned thrust, a reaction control system has been installed onboard the demonstrator. Another reason for the employment of the RCS is the impossibility of using the aerodynamic control surfaces of the vehicle to control it during the transatmospheric flight, i.e. where the air density is too low. Figure 13 illustrates the RCS system's architecture.

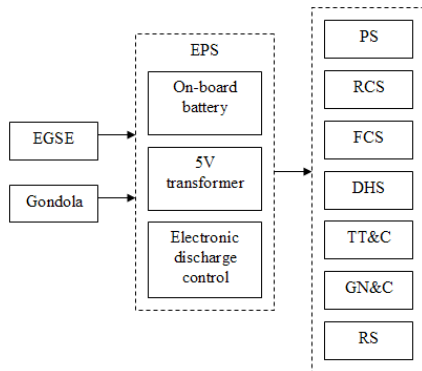


Fig. 12: EPS

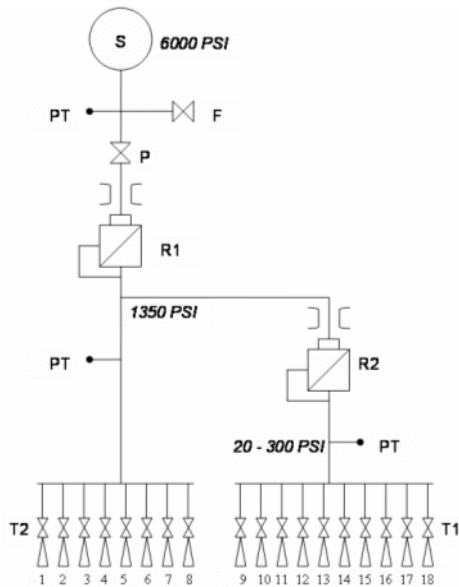


Fig. 13: RCS architecture

The propellant is stored in a titanium tank (S) at 6000 psi. The gas pressure is reduced to 1350 psi by a first pressure regulator (R1) to feed the block of thrusters T2 (25 N Thrusters), used for vehicle attitude control during the ascent boosted phase (continuous mode thrusting). A second pressure regulation, down to 300 psi, is performed by a second pressure regulator (R2) to feed the block of thrusters T1

(1 N thrusters), used for attitude control during the ballistic phases of the mission (pulsing mode thrusting). It should be remarked that the tank in the RCS schematic is spherical, but the tank selected to be integrated on board the vehicle is cylindrical (see figure 11) since this geometrical shape fits better inside the vehicle. Figure 14 shows the internal layout of the RCS thrusters: please note that the eight bigger thrusters (red in the figure) are the ones dedicated to attitude control during the boosted phase, while the other ten thrusters (black in the figure) are the ones dedicated to the attitude control during the ballistic flight.

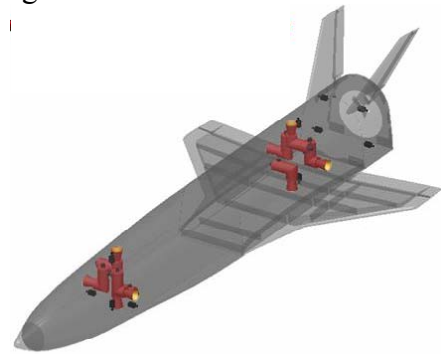


Fig. 14: internal layout of the RCS thrusters

6.4 Flight control system

During the atmospheric flight the demonstrator's attitude control is guaranteed by the aerodynamic surfaces: two elevons are dedicated to the roll control, if moved asymmetrically, and to the pitch control, if moved symmetrically, whereas the two aerodynamic surfaces of the butterfly tail allow the yaw control, if moved both to the same side, and the pitch control, if moved to opposite sides. All aerodynamic control surfaces are actuated by three DC electrical motors: one actuates both rudders and the others actuate the elevons, as shown in figure 15.

6.5 Other systems

6.5.1. Data Handling System and Tracking Telecommunication and Control System

The Data Handling System is composed by sensors and by one telemetry modular encoder,

which sends data via to the TT&C system serial interface. The telemetry system works as a real-time transmission. The tracking is performed by the transmission of an IFF signal, in accordance with the IFF requirements and procedures. The demonstrator can also be controlled from a ground station to guarantee safe abort for emergency procedures.

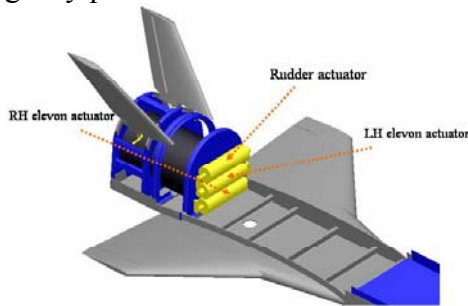


Fig. 15: Flight control system's electrical actuators

6.5.2. Guidance Navigation and Control System

Figure 16 illustrates the GN&C System's architecture. The GN&C system must perform autonomous Guidance, Navigation and Control during all the mission phases. GN&C functions to be carried out onboard Mini-FTB are ensured by:

- GN&C Software, which implements navigation, guidance and control algorithms and runs in the onboard computer;
- the GN&C computer;
- the GN&C sensors, whose function is to measure the vehicle navigation state (position, velocity and attitude). They include the following hardware:
 - the Integrated Inertial Navigation Unit (INS);
 - the GPS receiver;
 - three-axis fluxgate Magnetometer.

6.5.1. Recovery system

The Mini-FTB is equipped with a recovery system, based on a double staged not guidable parachute. The entire parachute system has to be contained in a cylinder of three liters of volume, closed by a removable panel, with three attachments points. That cylinder is located in the rear part of the demonstrator, mounted axially to the fuselage (figure 17). The proposed solution allows:

- the power system to be easily and precisely installed and safely separated by means of a Marmor belt;
- the demonstrator to be airtight and watertight after the parachute has been extracted.

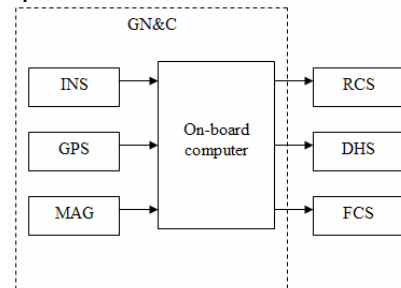


Fig. 16: GNC System architecture

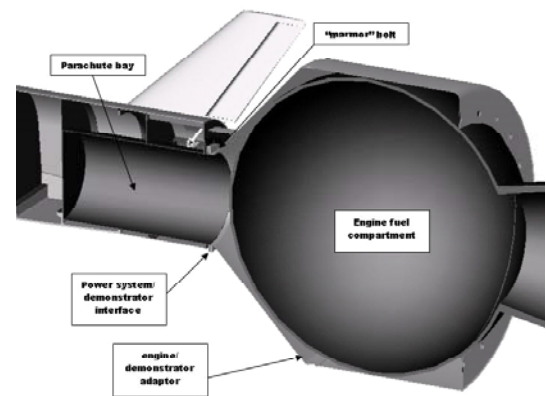


Fig. 17: recovery and power system CAD model

According to the mission requirements, the parachute must be opened at mach 0.6 and at a height of 10000 m. It must be a sequential opening: before a pilot chute and then a main chute. A rocket system has to be used for extraction. In compliance with the systems requirements, the maximum force at deployment must be less than 75 kN.

7 Weight estimation

Table 3 shows the weights breakdown for Mini-FTB, considering both options (Nitrogen and Freon 14) for the cold gas of the RCS System, while table 4 shows the weights breakdown for Mini-FTB/A, considering only the Freon 14 cold gas for the RCS System.

Structure (no optimisation):	27 kg
RCS (Nitrogen):	10.6 kg, 7.4 kg (dry)
RCS (Freon 14):	18 kg, 8.9 kg (dry)

Other systems:	12.2 kg
Payload:	2 kg
Mini-FTB (Nitrogen):	51.8 kg, 48.6 kg (dry)
Mini-FTB (Freon 14):	59.2 kg, 50.1 kg (dry)
Mini-FTB + power system (Nitrogen)	136 kg
Mini-FTB + power system (Freon 14)	143 kg

Tab. 3: Mini-FTB weights breakdown

Structure (no optimisation):	27 kg
RCS (Freon 14):	17.1 kg, 8.5 kg (dry)
Other systems:	12.2 kg
Payload:	2 kg
Mini-FTB (Freon 14):	58.3 kg, 49.7 (dry)
Mini-FTB + power system (Freon 14)	189 kg

Tab. 4: Mini-FTB/A weights breakdown

8 Aerothermodynamics

Aim of the paragraph is the presentation of the aerothermodynamic analysis results, in particular the investigation of the heat flux at stagnation point at nose and at wing leading edge. For this purpose analytical and computational methods have been employed. In particular the Fay-Riddell formula [7] and Fluent® software have been used. Conductive heat transfer is assumed to be negligible. Thus, the two main heat transfer mechanisms occurring onboard the vehicle are radiation and convection. Assuming convective heating to be the major source of energy input, the entry vehicle surface will continue to heat until the point where energy dissipation due to thermal radiation exactly balances the convective input.

8.1 Analytical analysis results

As at the beginning of the project the guidance law was not available, a performance's simulation program was first used to calculate the vehicle's trajectory. Applying the Fay-

Riddell formula to the reference trajectory, the graph of the heat flux density at stagnation point at nose versus time and the graph of the altitude versus time were obtained (figure 18). The same parameters were calculated for the wing leading edge. The most critical condition is highlighted in figure 18: it obviously corresponds to the highest heat flux of about 350 kW/m². Figure 19 illustrates the variation of the heat flux density versus time for two different configurations of Mini-FTB: the thicker line corresponds to the case of the nose radius drawn to 1:5 scale (same case of figure 19), while the thinner line corresponds to the case of the nose radius drawn to 1:1 scale. As can be noted the latter case presents more severe conditions than the former, but it meets mission requirements.

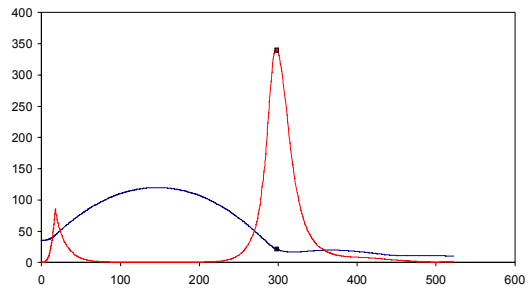


Fig. 18: Variation of altitude (km) with time (seconds) (blue line) and variation of heat flux density at nose (kW/m²) with time (seconds) (red line)

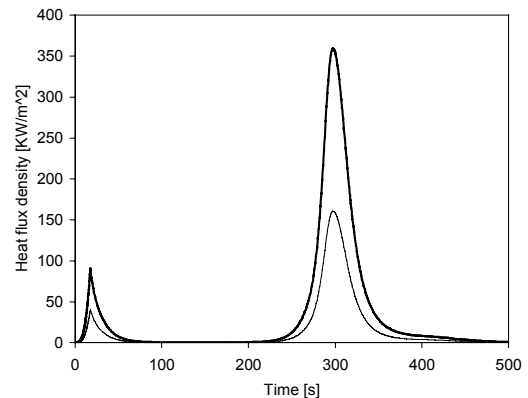


Fig. 19: heat flux density versus time for the Mini-FTB (nose radius drawn to 1:5 and 1:1 scale)

Figure 20 shows the variation of the heat flux density versus time for the Mini-FTB/A: the two configurations considered are the same as the ones in figure 19. The critical conditions have been investigated by extensive aerothermodynamic analyses carried out by the use of CFD programs (FLUENT®), under the

supervision of a research group at DENER, Politecnico di Torino.

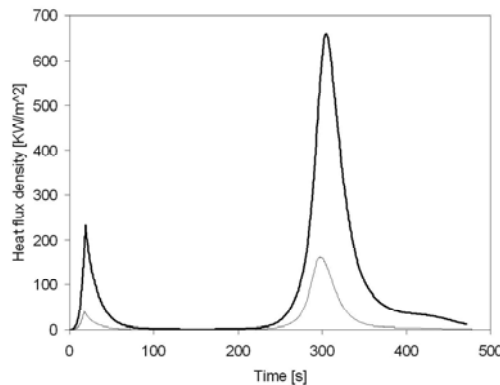


Fig. 20: heat flux density versus time for the Mini-FTB/A (nose radius drawn to 1:5 and 1:1 scale)

8.2 CFD analysis results

For easy of work and calculus, the demonstrator's nose has been considered as an axis-symmetric body, thus implying that the angles of incidence of the external flux have to be assumed equal to zero. Angles of incidence of the external flux different from zero imply an apparent radius of curvature at stagnation point bigger than the real one. Although considering angles of incidence of the external flux equal to zero simplifies the problem, it does also help validate the analytical analysis. Figure 21 illustrates the variation of the heat flux along the body longitudinal axis for the demonstrator's nose and front part. As can be noticed, the heat flux at the stagnation point is 168 kW/m^2 . Comparing this value to the result of the analytical analysis, 172 kW/m^2 (see figure 20, thinner line), it is possible to note that the difference is small, thus validating the analytical analysis. Figure 22 illustrates the variation of the surface temperature along the body longitudinal axis for the demonstrator's nose and front part.

9. Cost estimation, future activities and conclusions

Leaving the cost of the booster out, it is possible to assert that the total cost of the demonstrator is mainly due to the RCS system

(see figure 23). Taking into account the goal of reducing the whole system's cost, another vehicle's configuration has been conceived (figure 24). As already mentioned, the most expensive systems installed onboard the demonstrator are represented by the RCS and the power system, because they are both space qualified components. In order to achieve the required performance, a booster has to be used. COTS booster, manufactured for advanced experimental rocketry purpose, do exist and can be utilized, thus implying cost reduction and just a modest decreasing of performance. As far as the RCS is concerned, its employment is not mandatory but it depends on the mission profile.

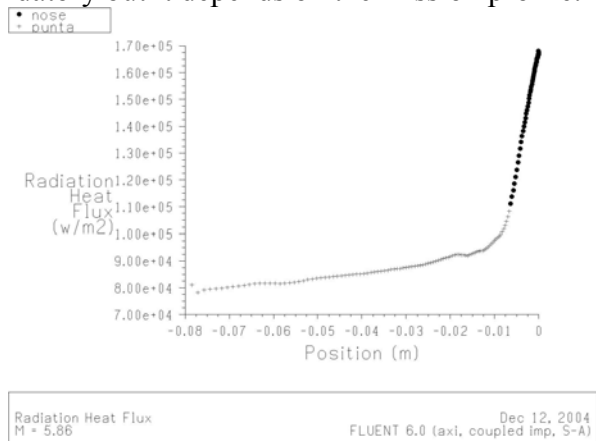


Fig. 21: variation of the heat flux along the body longitudinal axis for the demonstrator's nose (drawn to 1:1 scale) and front part

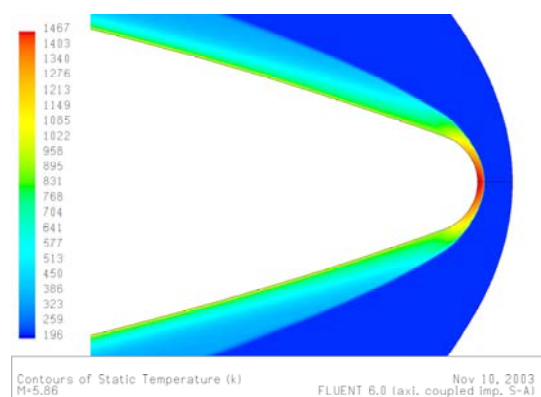


Fig. 22: variation of the surface temperature along the body longitudinal axis for the demonstrator's nose (drawn to 1:1 scale) and front part

The reference trajectory of the low-cost technological demonstrator does not require the use of the RCS system as the aerodynamic surfaces can be utilized for maneuvering and

controlling purposes during all flight, which extends up to a maximum altitude of about 70 km. It is obvious then that Mini-SRT sub-orbital ceiling height requirement is disappointed but the total cost of the project is substantially lower (figure 23). Unlike Mini-SRT mission, the separation between the demonstrator and its booster can now be delayed until re-entry to let the rear empennages of the booster's body help guarantee a desired stability margin. In order to further reduce system's complexity and cost, the demonstrator can be designed and manufactured as not reusable: in this way both the parachute system and the recovery operations can be avoided.

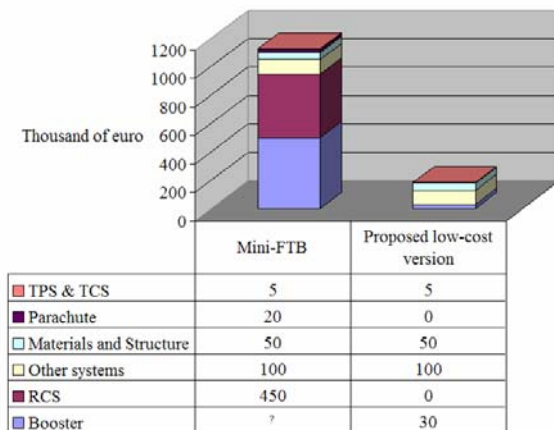


Fig. 23: first approximate cost estimation: Mini-FTB compared to a low-cost version of the demonstrator

Main advantages of the proposed low-cost demonstrator's configuration are:

- the possibility of keeping the project's cost down, thus making the demonstrator's design and manufacture affordable also for Universities budget;
- the capability of meeting at least few of the requirements of the mini-SRT mission, like testing the GN&C system and control laws in hypersonic flight regime.

Drawback of the proposed low-cost demonstrator's configuration is:

- the impossibility of meeting all Mini-SRT requirements.

To conclude it can be said that the present study has demonstrated the feasibility of Mini-FTB, as conceived to perform Mini-SRT mission. Its manufacture and test could surely

be a decisive factor for the FTB_2 and SRT mission's success.

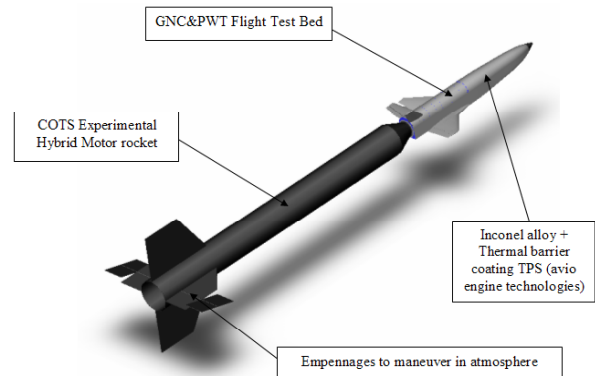


Fig. 24: Low-cost technological demonstrator

Acknowledgements

The authors are very grateful to Ing. F. Remiti for his precious contribution.

References

- [1] Russo G.. Next generations space transportation systems. *Aerotecnica-Missili e Spazio*, Vol 81 n°2, 2002.
- [2] Chiesa S., Camatti D., Corpino S., Pasquino M., Viola N.. Affordable technological demonstrator for hypersonic flight. *Fourth International Seminar on RRDPAE*, Warsaw, Poland, Vol. 4, 2000.
- [3] Chiesa S., Corpino S., Pasquino M., Viola N., Fiorio G., Milanese M., Masoero M., Silvi C.. Studio di fattibilità per un dimostratore tecnologico estremamente economico di velivoli ipersonici. *XVI National Congress AIDAA*, Palermo, Italy, Vol. XVI, 2001.
- [4] Chiesa S., Corpino S., Sembenini G., Viola N.. New hypothesis about hypersonic technological demonstrator based on standard air-to-air missiles. *53rd International Astronautical Congress*, Houston, Texas, Vol. 53, 2002.
- [5] Politecnico di Torino, Università di Napoli Federico II, Università di Roma La sapienza. *Mini-SRT feasibility study- Technical final report*. April 2004.
- [6] Remiti F.. *Studio di fattibilità di un dimostratore tecnologico sub-orbitale di dimensioni ridotte*. Final project in Aerospace Engineering, Politecnico di Torino, July 2003.
- [7] Hankey W.L.. *Re-entry Aerodynamics*. AIAA education series.